Measurement of Høgdahl neutron flux parameters in the SM1 subcritical reactor of the University of Pavia

Measurement of Høgdahl neutron flux parameters in the SM1 subcritical reactor of the University of Pavia

M Di Luzio[a,*], G D'Agostino[a], M Oddone[a,b]

[a] *c/o Unit of Radiochemistry and Spectroscopy, University of Pavia, Istituto Nazionale di Ricerca Metrologica (INRIM), via Taramelli 12, 27100 Pavia, Italy*
[b] *Department of chemistry, University of Pavia, via Taramelli 12, 27100 Pavia, Italy*

Abstract

Neutron flux of the thermal subcritical multiplication complex located at the nuclear pole of the University of Pavia was investigated to acknowledge the flux characteristics according to the Høgdahl convention in order to predict the expected activity of radionuclides while performing neutron activations. Flux parameters were measured by means of bare multi-monitor methods by preparing samples containing Au, Cr, Zn and Ni that were used to measure the epithermal shape correction factor, the conventional thermal to epithermal ratio and the thermal, epithermal and fast neutron fluxes in two irradiation channels of the facility.

Despite high uncertainties affecting epithermal shape correction factors, the thermal to epithermal ratio was measured with uncertainties ranging between tens and a few percent. In addition, conventional neutron fluxes were individually determined with a few percent level uncertainties, which are also suitable in applications requiring a known and/or ultra-stable neutron exposure.

Keywords: subcritical reactor, flux measurement, bare triple-method, Høgdahl convention

1. Introduction

Subcritical reactor assemblies are nuclear facilities producing neutrons without achieving criticality, thus the reaction is sustained with the aid of an external source; these reactors are highly appreciated for their safety and represent a valuable tool in the fields of research, training, education and nuclear waste management [1, 2].

The nuclear pole of the University of Pavia includes, alongside the 250 kW TRIGA Mark II reactor, a subcritical assembly installed in 1962 and provided with a Pu-Be source. This facility, called Subcritical Multiplication complex 1 (SM1), reports a licensed multiplicative coefficient value, k_{eff}, of 0.86, confirmed by the neutron flux characterization performed in 2013 using both foil standards activation with spectrum deconvolution and Monte Carlo simulations [3].

The choice of the external Pu-Be source offers significant advantages in terms of stability of the delivered neutron spectrum; in fact, the shape of neutron flux is unaffected by the grain size of Pu-Be and long term stability is guaranteed due to the

*Corresponding author
Email address: m.diluzio@inrim.it (M Di Luzio)

2.4×10^4 y half-life of ^{239}Pu [4]. On the other hand, the intensity of the neutron flux produced by a subcritical reactor is rather low with respect to critical nuclear reactors, even by many orders of magnitude.

Since the neutron profile of a subcritical reactor is a combination of fission spectrum of fuel elements and the spectrum of the external neutron source, its shape is influenced by the choice of nuclides adopted to produce neutrons as well as by fuel configuration and distance from the source position, due to the presence of moderator and reflector [5, 6]. The SM1 facility uses water as moderator. Since the Pu-Be source is known to produce a neutron spectrum similar to that of ^{235}U fission, a neutron profile somehow close to a typical water moderated critical reactor is expected according to a study reported on a similar assembly [1].

Despite the low flux intensity, a subcritical reactor might potentially be used in Neutron Activation Analysis (NAA) experiments while investigating elements in the range from macro constituents to sub-percent level, especially on environmental samples [7]; consequently, the knowledge of flux parameters is beneficial for what concerns the experimental design and uncertainty evaluation of relative-NAA investigations.

Following evidences and perspectives previously reported and also aiming at testing the limits for the use of SM1 as a neutron source for NAA, we decided to measure the neutron flux parameters by application of the Høgdahl convention in a similar way we already performed on the TRIGA Mark II reactor [8]. Specifically, the bare triple-monitor method [9], using a set of flux monitors containing Au, Cr, Zn and Ni, was adopted in order to investigate the epithermal shape correction factor, the conventional thermal to epithermal ratio and the thermal, epithermal and fast neutron fluxes in four positions of the two available irradiation channels (two spots each channel). The choice of the uncommon Au, Cr and Zn triple monitor set was driven by the nature of SM1 reactor and experimental setup. Due to the low neutron flux available the use of Zr was envisaged, due to its expected unsatisfactory activation, thus the alternative but equally suitable Au, Mo, Rb, Zn monitor set [10] was considered. The final set was completed by substituting Cr to Mo and Rb since they were discarded for the same reason of Zr as unsatisfactory activity was expected following irradiation with SM1 flux. In addition, two monitor samples were placed per irradiation channel in order to identify possible flux parameters trends along the facility.

2. Measurement models

Neutron flux parameters might be obtained from the knowledge of nuclear parameters and amounts of selected flux monitor elements and the outcome of γ-spectrometry countings performed on them. In this study, parameters accounting for the epithermal shape correction factor, α, thermal to epithermal conventional flux ratio, f, conventional thermal flux, Φ_{th}, and epithermal flux, Φ_{e}, are measured by application of a bare triple-monitor method while the conventional fast flux, Φ_{f}, is obtained by a bare single-monitor method. In this study we adopt the measurement equations used for a recent neutron flux characterization performed on a TRIGA Mark II reactor and reported in [8]. The theoretical basis and broad discussions can be found elsewhere [9].

The bare triple-monitor method allows to numerically calculate α while simultaneously irradiating a set of three $1/v$ monitors and counting the corresponding γ-emissions assuming that the flux parameters, addressed with Høgdahl convention, remain constant at the monitors' position during the irradiation.

In details, α is obtained by solving the following implicit equation using Au, Cr, Zn as monitors 1, 2 and 3, respectively.

$$\left(\frac{1}{\frac{A_{\mathrm{sp},1}k_{\mathrm{sa},2}k_{0,\mathrm{Au}}(2)\varepsilon_2}{A_{\mathrm{sp},2}k_{\mathrm{sa},1}k_{0,\mathrm{Au}}(1)\varepsilon_1}-1}-\frac{1}{\frac{A_{\mathrm{sp},1}k_{\mathrm{sa},3}k_{0,\mathrm{Au}}(3)\varepsilon_3}{A_{\mathrm{sp},3}k_{\mathrm{sa},1}k_{0,\mathrm{Au}}(1)\varepsilon_1}-1}\right)$$
$$\times G_{\mathrm{e},1}Q_{0,1}(\alpha)-\left(\frac{1}{1-\frac{A_{\mathrm{sp},2}k_{\mathrm{sa},1}k_{0,\mathrm{Au}}(1)\varepsilon_1}{A_{\mathrm{sp},1}k_{\mathrm{sa},2}k_{0,\mathrm{Au}}(2)\varepsilon_2}}\right)G_{\mathrm{e},2}Q_{0,2}(\alpha) \tag{1}$$
$$+\left(\frac{1}{1-\frac{A_{\mathrm{sp},3}k_{\mathrm{sa},1}k_{0,\mathrm{Au}}(1)\varepsilon_1}{A_{\mathrm{sp},1}k_{\mathrm{sa},3}k_{0,\mathrm{Au}}(3)\varepsilon_3}}\right)G_{\mathrm{e},3}Q_{0,3}(\alpha)=0,$$

where $A_{\mathrm{sp},i}$ is the specific count rate at saturation, $k_{\mathrm{sa},i}$ is the γ self-absorption correction factor, $k_{0,\mathrm{Au}}(i)$ is a composite nuclear constant known as k_0 factor, ε_i is the γ full-energy peak detection efficiency, $G_{\mathrm{e},i}$ is the epi-cadmium neutron self-shielding factor, $Q_{0,i}(\alpha)$ is the effective resonance integral to thermal cross section ratio taking into account the effect of α.

It is worth to note that, the use of monitors emitting gammas through (n,γ) non-complex activation decay paths not affected by true-coincidence summing requires the application of eq. (2) to evaluate A_{sp}:

$$A_{\mathrm{sp}}=\frac{(n_{\mathrm{p}}\,\lambda\,t_{\mathrm{c}})}{t_{\mathrm{l}}\,(1-e^{-\lambda t_{\mathrm{i}}})\,e^{-\lambda t_{\mathrm{d}}}\,(1-e^{-\lambda t_{\mathrm{c}}})\,w}, \tag{2}$$

where n_{p} is the full-energy peak net area, λ is the decay constant, t_{c} is the (real) counting time, t_{l} is the (live) counting time, t_{i} is the irradiation time, t_{d} is the decay time spanning from irradiation end to start counting, w is the mass of monitor element.

The measured α value is then used to evaluate f according to:

$$f=\frac{\frac{k_{0,\mathrm{Au}}(1)\varepsilon_1}{k_{0,\mathrm{Au}}(2)\varepsilon_2}G_{\mathrm{e},1}Q_{0,1}(\alpha)-\frac{A_{\mathrm{sp},1}k_{\mathrm{sa},2}}{A_{\mathrm{sp},2}k_{\mathrm{sa},1}}G_{\mathrm{e},2}Q_{0,2}(\alpha)}{G_{\mathrm{s}}\left(\frac{A_{\mathrm{sp},1}k_{\mathrm{sa},2}}{A_{\mathrm{sp},2}k_{\mathrm{sa},1}}-\frac{k_{0,\mathrm{Au}}(1)\varepsilon_1}{k_{0,\mathrm{Au}}(2)\varepsilon_2}\right)}, \tag{3}$$

where G_{s} is the sub-cadmium neutron self-shielding correction factor.

Successively, Φ_{th} and Φ_{e} and Φ_{f} are evaluated using Au monitor for the formers and Ni monitor for the latter parameter.

$$\Phi_{\mathrm{th}}=\frac{A_{\mathrm{sp}}\,M}{\theta\,\Gamma\,\varepsilon\,k_{\mathrm{sa}}\,N_{\mathrm{A}}\,\sigma_0\left(G_{\mathrm{s}}+G_{\mathrm{e}}\frac{Q_0(\alpha)}{f}\right)}, \tag{4}$$

$$\Phi_{\mathrm{e}}=\frac{A_{\mathrm{sp}}\,M}{\theta\,\Gamma\,\varepsilon\,k_{\mathrm{sa}}\,N_{\mathrm{A}}\,\sigma_0\,(G_{\mathrm{s}}f+G_{\mathrm{e}}Q_0(\alpha))}, \tag{5}$$

$$\Phi_{\mathrm{f}}=\frac{A_{\mathrm{sp}}\,M}{\theta\,\Gamma\,\varepsilon\,k_{\mathrm{sa}}\,N_{\mathrm{A}}\,\sigma_{\mathrm{f}}}, \tag{6}$$

with M the molar mass of monitor element, θ the isotopic fraction of target isotope, Γ the emission γ-yield, N_{A} the Avogadro constant, σ_0 the thermal cross section and

σ_f the ^{235}U fission-neutron averaged cross section accounting for the ^{58}Ni(n,p)^{58}Co reaction, respectively.

It is worth to note that Φ_{th} and Φ_e, calculated with bare triple-monitor method, heavily rely on the previous determinations of f and, in turn, α. Moreover, the combined uncertainty is also evaluated by propagating variances through the measurement models here reported by taking into account correlations among parameters.

3. Experimental

3.1. Irradiation facility

SM1 is assembled in a hexagonal prism core configuration with fuel elements immersed in light water and consisting of natural uranium in metallic form. The external shielding of the core tank is made of aluminum filled up with paraffin. See the schematic draw in figure 1a.

The current configuration counts 206 aluminum-clad fuel elements assembled in an hexagon with inscribed and circumscribed diameters of 59.0 cm and 68.2 cm, respectively. Each fuel element is filled with five cylindrical metallic uranium ingots (2.74 cm diameter and 21.5 cm length of approximately 2 kg mass, per ingot). The Pu-Be neutron hollow cylindrical source (2.0 cm internal diameter, 5.2 cm external diameter and 5.0 cm height), emitting with an activity of 8.9×10^6 Bq, is placed at the center of the hexagonal prism where two irradiation channels are currently available: the internal one is inserted in the conventionally called Ring-2 and is placed at a distance of 6.2 cm from the axis of the neutron source, the external one lies in the Ring-7 and is placed at a distance of 24.3 cm from the source. Samples are usually irradiated in a polyethylene (PE) irradiation container (8.7 cm and 2 cm internal height and diameter, respectively) placed within the core by a plexiglass rod. The mid-point vertical position of the irradiation containers is horizontally aligned with the Pu-Be source, as shown in figure 1b, as well as with the central ingot of the fuel elements.

3.2. Preparation and neutron exposure of monitor samples

In this study we carried out two different experiments using two sets of four samples, one for the measurement of α, f, Φ_{th} and Φ_e and one for the measurement of Φ_f.

The first sample set consisted of solutions containing Au, Cr and Zn prepared from liquid and solid standards. In particular, amounts of approximately 210 mg of Zn powder (Sigma Aldrich, 99.998 % purity) were placed in four 3 mL PE irradiation vials and weighted on an analytical balance traceable to SI; the Zn powder was dissolved in 1 mL of a HNO_3 solution. A mass of 13.8716(2) g of a Au standard solution (Sigma Aldrich, 999(1) μg mL^{-1} concentration and 1.0256(5) g mL^{-1} density) was concentrated by evaporation to reach a final solution mass of 1.6855(2) g; the final Au mass fraction was $8.016(8) \times 10^{-3}$ g g^{-1}. Here and hereafter, values in parenthesis indicate the standard uncertainty and refer to the last digits. Aliquots of about 400 μL of the Au concentrated solution were weighted and added to the four sample irradiation vials. As a final step, about 150 mg masses of $K_2Cr_2O_7$ powder (Carlo Erba 99.5 % purity) were weighted and dissolved in the four irradiation vials. Sample solutions were finally diluted by addition of deionized water to reach volumes of 2 mL with 1.6 cm height. It is worth to note that, since considerable volumes of liquid were weighted, the loss of mass due to evaporation was negligible with negligible effect on the measurement uncertainty.

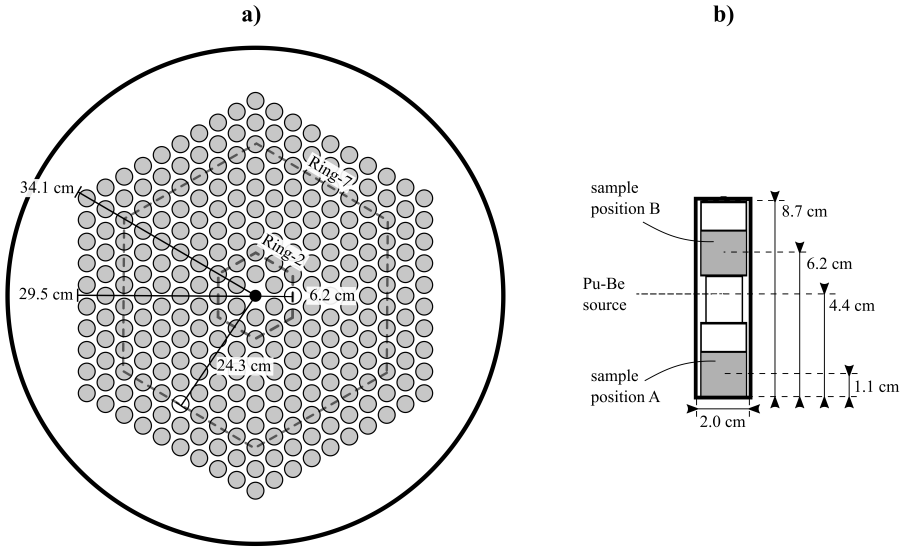

Figure 1: Schematic horizontal cross section of the SM1 reactor **a)** and sample positions within the irradiation container with distances **b)**. In **a)** the Pu-Be source and irradiation channels are indicated by a black dot and white circles, respectively.

The Au, Cr and Zn monitor vials were finally heat-sealed to avoid loss of solution, vertically placed into the irradiation containers and located within Ring-2 and Ring-7 channels at the positions A and B which mid-points of the liquid lie at 1.1 cm and 6.2 cm distance from the irradiation container bottom, respectively; see figure 1b for sample positioning. The irradiation lasted 89 days and 139 days for the monitors in Ring-2 and in Ring-7, respectively.

The second sample set consisted of solutions containing Ni to exploit the fast neutron reaction ^{58}Ni(n,p)^{58}Co and prepared from a solid standard. In particular, a 3.5483(1) g mass sample of a Ni foil was dissolved in HNO_3 to obtain a final solution of 18.7834(2) g with Ni mass fraction of 0.188 90(1) g g^{-1}. Aliquots of 2 mL of the Ni solution were pipetted and weighted in four 3 mL PE irradiation vials to obtain samples with 1.6 cm height.

The Ni monitor vials were heat-sealed, placed into the irradiation containers and located within the channels for irradiation. The irradiation lasted 56 days and 62 days for the monitors in the Ring-2 and in Ring-7, respectively. Great care was adopted in order to place the Ni monitors at same position of the Au, Cr and Zn solutions in the previous irradiation.

In both activation experiments, irradiation times for samples in Ring-2 were shorter than those in Ring-7 depending on the lower neutron flux expected in the latter channel. Unfortunately, the stability of neutron flux during monitors irradiation was not checked online.

3.3. Gamma spectrometry measurements

Monitor irradiation vials were extracted from irradiation containers, directly placed at the center of plastic circular containers for γ-counting and measured with a ORTEC GEM-S8530P4 HPGe detector (50 % relative efficiency, 1.64 keV FWHM at 1332.5 keV energy) connected to an ORTEC DSPEC 502 multi-channel analyzer.

Counting containers were positioned in contact with the detector end-cap. The detection system was calibrated in energy and efficiency using a certified multi-γ source issued by Laboratoire d'Etalon d'Activité (LEA) with code 12ML01EGMA15; the efficiency calibration was performed with the multi-γ source at a distance of 1.0 cm from the detector end-cap, i.e. the mid-point distance between the bottom (0.2 cm) and the top (1.8 cm) distance of the monitor sample solution from the end-cap. Due to the close counting distance, only the 10 available true-coincidence free emissions were adopted for the efficiency fit.

Eight spectra were collected for Au, Cr and Zn monitor samples: four short countings ranging from 0.23 days to 1.10 days to acquire the ^{198}Au 411.8 keV full-energy peak and four long countings ranging from 4.8 days to 25.6 days to acquire the ^{51}Cr 320.1 keV and ^{65}Zn 1115.5 keV full-energy peaks. Four spectra were acquired for Ni monitor samples ranging from 1.7 days to 10.1 days to collect the ^{58}Co 810.8 keV full-energy peak. Acquisition times were online adjusted to reach counting uncertainties of 1.6 % and 0.6 % for monitors irradiated at Ring-7 and Ring-2, respectively. Recorded relative dead times were always below 0.1 %, close to the expected value for an environmental background acquisition.

4. Results and discussion

Collected γ-spectra were processed using the moderate count rate and regular peaks algorithm of the HyperLab software to calculate the net area of the γ-peaks.

Several input parameters were retrieved from literature: in particular, k_0, σ_0, Q_0, $\bar{E}_r$ and λ values, including their uncertainty, were taken from the k_0 database [11] while M_{Au}, θ_{Au}, Γ_{Au}, M_{Ni}, θ_{Ni}, Γ_{Co} and N_A values were retrieved from [12, 13, 14, 15]; the widely-accepted 0.111(3) b value of the ^{58}Ni fission spectrum averaged cross section, σ_f, was adopted [16].

Full-energy peak efficiencies, ε, for the relevant γ-emissions energies were calculated by application of an exponential four-terms polynomial function [17] to fit the experimental data acquired with the certified multi-γ source. Correction factors accounting for k_{sa}, G_s and G_e, respectively, were considered close to the unity with negligible uncertainty due to the dilution of the monitors in solutions.

Moreover, in order to exclude a possible neutron flux thermalizing effect due to the water in the 2 mL solutions a further irradiation of Au monitors was performed. In particular, a thin disc (12 mm diameter) and a 2 mL solution (obtained by dissolution of a further monitor disc) were respectively placed in positions A and B of the irradiation channel within Ring-2; a second couple of Au monitors with same configuration was also adopted in Ring-7. The irradiation lasted 14 days for the Ring-2 samples and 20 days for the Ring-7 samples. The resulting specific count rates for Au evaluated with eq. (2), with estimated uncertainty of 2.5 % mainly due to sample positioning during γ-counting, were normalized with respect to the specific count rate values of liquid Au monitor placed in position B. The resulting normalized trends were compared with the similarly normalized specific count rate trends measured for Au in the multi-monitor experiment for the corresponding irradiation channels. The comparison highlighted agreement of the trends within the stated uncertainty. This comparison supports the thesis of a negligible (within the stated uncertainty) thermalizing effect due to the water in monitor solution in the particular setup adopted in this work. The comparison of normalized specific count rates was necessary to reduce uncertainty and exclude γ-counting biases since the Au monitor were counted on a less efficient detector (35 % relative efficiency) with respect to that used to acquire the multi-monitors of this study.

Results were obtained by applying equation models recalled in the paragraph 'Measurement models'. Uncertainties of α, f, Φ_{th}, Φ_e and Φ_f were evaluated in agreement with the low of uncertainty propagation for correlated input parameters as reported in the Guide to expression of Uncertainty in Measurement (GUM) [18]. To this aim, covariances, related to correlated parameters, were obtained by the adopted fitting algorithms whereas sensitivity coefficients were evaluated by accounting for perturbations of the measurement model induced by variation of input parameters, for any parameter of the considered equation; finally, covariances and sensitivity coefficients were propagated to calculate the corresponding combined uncertainties. Data are shown in table 1.

Table 1: Measured values of α, f, Φ_{th}, Φ_e, and Φ_f in positions A and B of the irradiation channels Ring-2 and Ring-7. Values in parenthesis indicate the standard uncertainty and refer to the last digits.

Channel	Position	α / 1	f / 1	Φ_{th} / cm^{-2} s^{-1}	Φ_e / cm^{-2} s^{-1}	Φ_f / cm^{-2} s^{-1}
Ring-2	A	−0.010(70)	16.7(21)	$2.12(18) \times 10^4$	$1.27(11) \times 10^3$	$1.92(7) \times 10^4$
	B	−0.031(27)	16.4(12)	$2.42(11) \times 10^4$	$1.48(7) \times 10^3$	$2.90(10) \times 10^4$
Ring-7	A	−0.019(11)	19.4(37)	$3.89(48) \times 10^3$	$2.00(27) \times 10^2$	$1.52(6) \times 10^3$
	B	−0.030(88)	20.1(32)	$4.22(43) \times 10^3$	$2.10(24) \times 10^2$	$1.56(6) \times 10^3$

There is evidence that the knowledge of α values is limited by the uncertainties largely exceeding the 100 % level. The investigation of uncertainty budgets for α values indicates that the predominant contribution is identified to be the efficiency evaluation; the reason might depend on the strong correlations existing among fitting parameters or on the non-linearity of the adopted equations that is, in this situation, exacerbated by the high uncertainty affecting the input parameters due to the non-trivial experimental setup. This evidence suggests that the measurement of the epithermal neutron shape following Høgdahl convention is challenging in subcritical reactors. Nevertheless, relative uncertainties evaluated for the f values, mainly due to α, are below 12 % and 20 % in Ring-2 and Ring-7, respectively, proving that effect of α is limited on the measurement of the other flux parameters. The α and f are main contributors to the uncertainties of Φ_{th} and Φ_e. Specifically, relative uncertainties of Φ_{th} are below 9 % and 12 % in Ring-2 and Ring-7, respectively, while relative uncertainties of Φ_e are below 9 % and 14 % in Ring-2 and Ring-7, respectively. Finally, relative uncertainties achieved for Φ_f are about 4 % in all the investigated positions.

The expected reduction of the conventional fluxes from Ring-2 to Ring-7 is confirmed by the results. The average relative decreases of Φ_{th}, Φ_e and Φ_f are 82 %, 86 % and 93 %, respectively. Accordingly, the average relative increase of f is 20 % although the uncertainty affecting the measured parameters might also suggest the suspected discrepancy is merely random. No vertical variations of Φ_{th}, Φ_e and f are detected within the evaluated uncertainties both in Ring-2 and Ring-7. In addition, a 51 % relative increase of Φ_f occurs in about 5 cm height at Ring-2 whereas no vertical variations of Φ_f are identified within Ring-7.

Despite the core configuration differences, due to a rearrangement of irradiation channels, it might be interesting to compare the results obtained in this study with the integral neutron fluxes at Ring-2 and Ring-4 measured and reported in 2013 using foil standards activation with spectrum deconvolution [3]; in particular, we expected similar flux values for the Ring-2 since its position was moved closer to the neutron source by only few millimeters with respect to the previous configuration. To get a meaningful comparison, the conventional neutron fluxes were converted to their corresponding integral fluxes according to the definition of conventional fluxes described in [19]; the

resulting values must be taken as informative because we arbitrarily assumed $\alpha = 0$ and a neutron temperature $T_n = 20.44\,^{\circ}\mathrm{C}$. Data are reported in table 2.

Table 2: Integral fluxes, φ, measured in SM1 at Ring-2 and Ring-4 by foil activation and spectrum deconvolution in 2013 and at Ring-2 and Ring-7 by conversion of conventional fluxes in this work. Values in parenthesis indicate the standard uncertainty and refer to the last digits.

Channel	φ[3] / cm^{-2} s^{-1}	Channel	φ[this work] / cm^{-2} s^{-1}
Ring-2	$5.9(2) \times 10^4$	Ring-2	$6.9(6) \times 10^4$
Ring-4	$2.59(8) \times 10^4$	Ring-7	$9.0(17) \times 10^3$

Although the comparison is affected by channel position differences, the integral fluxes are reasonable since values in Ring-2 appear approximately compatible while they drop at the farthest irradiation channel, by 56 % and 87 % with respect to Ring-2 in the 2013 measurement and in this work, respectively. Actually, the flux measured at Ring-7 is considerably smaller compared to the datum collected at Ring-4 since the farthest irradiation channel lies now about 10 cm farther to the neutron source.

5. Conclusion

Neutron flux parameters based on Høgdahl convention were measured in two irradiation channels of the subcritical reactor complex SM1 installed in the University of Pavia. Although measured epithermal shape correction factors were affected by an extremely high uncertainty making them poorly meaningful, the uncertainties reached with the conventional thermal to epithermal ratios and the thermal, epithermal and fast neutron fluxes values are acceptably limited between tens of percent and a few percent levels. The negative trend of the conventional fluxes moving horizontally away from the source is significant whereas no vertical variations were observed in a few centimeters except for the fast neutron flux in the inner channel.

The neutron flux characteristics in the thermal, epithermal and fast regions are useful in applications requiring a known and/or ultra-stable neutron exposure. Due to the very low neutron flux level, the use of SM1 in elemental analysis performed by NAA is possible but limited to measurements where the investigated elements are major or at percent level. The measured flux parameters indicate that irradiated targets activate through thermal and epithermal neutrons with a similar ratio to that observed in the TRIGA Mark II reactor, but with 8 orders of magnitude less intensity.

Apart from analytical applications, the knowledge of flux parameters is still valuable to predict the expected activity produced following a neutron exposure in the SM1 facility.

6. References

[1] H R Vega-Carrillo, I R Esparza-Garcia, and A Sanchez. Features of a subcritical nuclear reactor. *Ann Nucl Energy*, 75:101–106, 2015. doi: 10.1016/j.anucene.2014.08.006.

[2] C-M Persson, P Seltborg, A Ahlander, W Gudowski, T Stummer, H Kiyavitskaya, V Bournos, Y Fokov, I Serafimovic, and S Chigrinov. Analysis of reactivity determination methods in the subcritical experiment Yalina. *Nucl Instr Meth Phys Res*, 554:374–383, 2005. doi: 10.1016/j.nima.2005.07.058.

[3] D Alloni, A Borio di Tigliole, J Bruni, M Cagnazzo, R Cremonesi, G Magrotti, M Oddone, F Panza, M Prata, and A Salvini. Neutron flux characterization of the SM1 sub-critical multiplying complex of the Pavia university. *Prog Nucl Energy*, 67:98–103, 2013. doi: 10.1016/j.pnucene.2013.04.004.

[4] L Stewart. Neutron spectrum and absolute yield of a plutonium-beryllium source. *Phys Rev*, 98:740–743, 1955.

[5] A Dall'Osso. The influence of the neutron source spectrum on the infinite homogeneous reactor in subcritical condition. *Ann Nucl Energy*, 77:408–414, 2015. doi: 10.1016/j.anucene.2014.12.006.

[6] N Xoubi. Calculation of the power and absolute flux of a source driven subcritical assembly using Monte Carlo MCNP code. *Ann Nucl Energy*, 97:96–101, 2016. doi: 10.1016/j.anucene.2016.07.009.

[7] M Manolopoulou, S Stoulos, and A Ioannidou. A subcritical nuclear reactor as neutron source for applying INAA in environmental samples, 2017. URL `https://inis.iaea.org/search/search.aspx?orig_q=RN:49053159`.

[8] M Di Luzio, G D'Agostino, M Oddone, and A Salvini. Vertical variations of flux parameters in irradiation channels at the TRIGA Mark II reactor of Pavia. *Prog Nucl Energy*, 113:247–254, 2019. doi: 10.1016/j.pnucene.2019.01.025.

[9] F De Corte, K Sordo-El Hammami, L Moens, A Simonits, A De Wispelaere, and J Hoste. The accuracy and precision of the experimental α-determination in the $1/E^{1+\alpha}$ epithermal reactor-neutron spectrum. *J Radioanal Nucl Chem*, 62: 209–255, 1981. doi: 10.1007/BF02517354.

[10] M Kubesova, I Krausova, and J Kucera. Verification of k_0-NAA results at the LVR-15 reactor in Rez with the use of Au+Mo+Rb(+Zn) monitor set. *J Radioanal Nucl Chem*, 300:473–480, 2014. doi: 10.1007/s10967-014-2991-7.

[11] k_0 database, 2018. URL `http://www.kayzero.com/k0naa/k0naaorg/Nuclear_Data_SC/Entries/2016/1/11_New_k0-data_Library_2015.html`.

[12] J Mejia, T B Coplen, M Berglund, W A Brand, P De Bievre, M Groning, N E Holden, J Irrgeher, R D Loss, T Walczyk, and T Prohaska. Atomic weights of the elements 2013. *Pure Appl Chem*, 88:265–291, 2016. doi: 10.1515/pac-2015-0305.

[13] H Xiaolong and K Mengxiao. Nuclear data sheets for A=198. *Nucl Data Sheets*, 133:221–416, 2016. doi: 10.1016/j.nds.2016.02.002.

[14] C D Nesaraja, S D Geraedts, and B Singh. Nuclear data sheets for A=58. *Nucl Data Sheets*, 111:897–1092, 2010.

[15] D B Newell, F Cabiati, J Fischer, K Fujii, S G Karshenboim, H S Margolis, E de Mirandes, P J Mohr, F Nez, K Pachucki, T J Quinn, B N Taylor, M Wang, B M Wood, and Z Zhang. The CODATA 2017 values of the h, e, k and N_A for the revision of the SI. *Metrologia*, 55:L13–L16, 2018.

[16] M A Arribere, S Ribeiro Guevara, P M Suarez, and A J Kestelman. Threshold reaction cross sections of nickel isotopes, averaged over a ^{235}U fission neutron spectrum. *Nucl Sci Eng*, 139:24–32, 2001.

[17] Z Kis, B Fazakas, J Ostor, Z Revay, T Belgya, G L Molnar, and L Koltay. Comparison of efficiency functions for Ge gamma-ray detectors in a wide energy range. *Nucl Instr Meth Phys Res A*, 418:374–386, 1998.

[18] BIPM. *Guide to the expression of uncertainty in measurement*. Bureau International de Poids et Mesures, 1993.

[19] F De Corte. *The k_0-standardization method. A move to optimization of neutron activation analysis*. University of Gent, 1987.